Geoarchaeological Simulation of Meandering River Deposits and Settlement Distributions: A Three-Dimensional Approach

Quintijn Clevis,[1],* Gregory E. Tucker,[1] Gary Lock,[2] Stephen T. Lancaster,[3] Nicole Gasparini,[4] Arnaud Desitter,[5] and Rafael L. Bras[6]

[1]*Cooperative Institute for Research in Environmental Sciences (CIRES) and Department of Geological Sciences, University of Colorado, Boulder, CO 80309-0216*

[2]*Institute of Archaeology, Oxford University, Oxford, OX1 2PG, United Kingdom*

[3]*Department of Geosciences, Oregon State University, Corvallis, OR 97331-5506*

[4]*Department of Geology and Geophysics, Yale University, New Haven, CT 06520-8109*

[5]*School of Geography and the Environment, Oxford University, Oxford, OX1 3QY, United Kingdom*

[6]*Department of Civil and Environmental Engineering, Massachusetts Institute of Technology, Cambridge, MA 02139*

Fluvial processes have the potential to obscure, expose, or even destroy portions of the archaeological record. Floodplain aggradation can bury and hide archaeological features, whereas actively migrating channels can erode them. The archaeological record preserved in the subsurface of a fluvial system is potentially fragmented and is three-dimensionally complex, especially when the system has been subjected to successive phases of alluviation and entrenchment. A simulation model is presented to gain insight into the three-dimensional subsurface distribution, visibility, and preservation potential of the archaeological record in a meander-floodplain system as a function of geomorphic history. Simulation results indicate that fluvial cut-fill cycles can strongly influence the density of archaeological material in the subsurface. Thus, interpretation of floodplain habitation based solely upon features visible in the shallow subsurface (through traditional techniques such as aerial photography and geophysical prospection) can be misleading. In the examples, the loss of archaeological record by channel migration ranges between 45% and 90% over 12,000 years for channel belt-dominated systems, decreasing to 10 to 30% for rivers where the floodplain width is a multiple of channel belt width. The modeling presented can be used to test excavation strategies in relation to hypothesized scenarios of stratigraphic evolution for archaeological sites. © 2006 Wiley Periodicals, Inc.

WILEY InterScience®
DISCOVER SOMETHING GREAT

INTRODUCTION

River systems are sensitive to changes in climate, vegetation, and human land-use patterns (Bull, 1991; Brown, 1997; Macklin and Lewin, 2003). Worldwide, many examples of changes in fluvial systems during the late Pleistocene and Holocene have been documented. Patterns of evolution include terrace formation in response to cyclic alluviation and entrenchment (e.g., Brakenridge, 1980; Johnson and Logan, 1990; Hancock and Anderson, 2002), changes in channel pattern from braided to meandering (Huisink, 1997), changes in position due to channel meandering and cut-offs, and periods of rapid floodplain burial or incision (Vandenberghe, 1995; Tebbens et al., 1999; Macklin and Lewin, 2003). These modes of river and floodplain response have implications for the three-dimensional (3D) subsurface distribution of fluvial deposits and the preservation potential of any archaeological materials they may contain. A fluvial system has the potential to obscure, expose, or even destroy portions of the fluvial and archaeological record. In valley systems with actively migrating channels, much material can be lost to lateral bank erosion, whereas floodplain aggradation can bury and, therefore, obscure archaeological features (Waters and Kuehn, 1996; Brown, 1997; Walker et al., 1997; Guccione et al., 1998; Waters, 2000). For example, Bettis and Mandel (2002) argue, based on a study of preserved alluvial chronologies, that cultural deposits of the Archaic period are rare in valley systems of central North America because these systems were dominated by erosion and net transport throughout much of the Holocene. The archaeology observed is, therefore, not a complete record of human activity, but a filtered record modulated by geologic processes. Furthermore, differential alluvial burial histories in different parts of a floodplain or terrace levels can introduce spatially varying degrees of archaeological preservation. When these environments are sampled using a limited excavation strategy, the results can lead to biased interpretations of the complete settlement pattern. In addition, these spatially complex patterns of archaeological preservation may overlap with occurrences of economically important resources, such as sand and gravel deposits. Integrating knowledge of the fluvial geoarchaeological environment into the development-control process has the potential to reduce the impact of resource extraction on the historic environment (Kerr, 2004).

Our objective in this article is to quantify and visualize the relationships between geomorphic history, fluvial subsurface architecture, and archaeological preservation potential with the aid of a process-based model for landscape development. For this purpose, the landscape evolution model, CHILD (channel hillslope integrated landscape model; Tucker et al., 2001b) was modified to record a 3D stratigraphic record created by a meandering river. In addition, to demonstrate the potential for coupled modeling of landscape evolution and human behavior, we deploy a very simple two-dimensional cellular-automata algorithm to represent settlement behavior and the creation of archaeological features. The settlement algorithms are deliberately naïve and designed simply to illustrate the potential for archaeological hypothesis testing using this method. The simulations presented provide visual templates for thinking about different potential forms of Holocene

valley evolution and archaeological preservation potential; they are not intended to reconstruct any specific field sites.

Process-based models of fluvial architecture are frequently used in geology to predict the 3D subsurface of floodplains for fluid-flow studies in aquifers and hydrocarbon reservoirs (Stølum and Friend, 1997; Gross and Small, 1998; Wen, 2004). Archaeological computer simulation in the form of agent-based modeling has been used to investigate the evolution of settlement patterns as a function of available natural resources and sociocultural characteristics. Well-known examples are the simulation of Prehistoric settlement systems in the American Southwest using the Swarm agent-based modeling libraries (Kohler and Gumerman, 2000), and the simulation of hunter–gatherer foraging (Lake, 2000). Statistical models of potential site distribution, based on observed correlation between known sites and various landscape attributes (e.g., proximity to water, topography, and depositional setting), have been used to supplement ground-based surveys (e.g., Johnson and Zeidler, 1999; Zeidler and Isaacson, 1999; White, 2000). Although some efforts have been made to use process-based models to improve our understanding of archaeological site formation and modification (Wainwright, 1994; Ward and Larcombe, 2003), the potential remains largely unexploited. In this article, we describe the first 3D model designed to couple both archaeological site formation and geomorphic change. The model serves to enhance understanding of river valley archaeology and geomorphology by quantifying and visually rendering the relationships between fluvial-geomorphic evolution and archaeological resource potential.

Specifically, we use simulation modeling as a platform for developing insight into the means by which geomorphic evolution can introduce systematic bias into the archaeological record. To that end, we model the geomorphic evolution of a hypothetical 5-km stretch of alluvial valley over a period of 12,000 years. Three different scenarios are analyzed, ranging from steady-state aggradation to rapid cut-fill cycles. By introducing a simple model of settlement dynamics that is linked to the evolving topography and hydrology, it becomes possible to compare, in a controlled framework, the difference between the actual settlement history and that implied by the accessible archaeological record. The results illustrate the potential archaeological implications of some common patterns in alluvial history.

METHOD

River Meandering and Floodplain Sedimentation

CHILD is a numerical model of erosion and sedimentation based on an adaptive triangular mesh, and can simulate landscape evolution in a river basin over periods ranging from centuries to epochs (Tucker et al., 2001a, 2001b; Clevis et al., 2006). Simulations are performed by numerically solving a set of partial differential equations for surface processes. The solution algorithms are embedded in a time loop and state variables (e.g., terrain height) are updated sequentially in small time steps. The lengths of these time steps and the intensity of the rainfall and stream flow are dictated by a storm module, which generates a series of storms at random from a

Poisson probability distribution (Eagleson, 1978). The runoff cascades down slope across the surface and is used to calculate erosion and deposition at different locations in the simulation landscape. The surface processes in the CHILD model have been described in detail by Tucker et al. (2001a, 2001b), and Tucker (2004). Here, we focus on the modules for river meandering, stratigraphy, and archaeological site burial. (Note that the term *site* is used here to mean collections of one or more related features or artifacts).

The meander module in CHILD uses a combination of simplified process physics and process-based rules to model channel evolution at time scales relevant to floodplain and terrace development (on the order of 1000–10,000 years; Lancaster and Bras, 2002; Lancaster, 1998). The meander model is based on the concept of topographic steering (Dietrich and Smith, 1983; Smith and McLean, 1984), which derives from the observation that secondary flows over the bed topography translate the erosive high-velocity core in a channel segment laterally. This secondary flow results in transfer of momentum and maximum shear stress toward the outer bank and downstream, causing erosion. The modeled rate of channel migration at a given point is defined by the rate of bank erosion, which is proportional to the bank shear stress:

$$R_{migration} = E\tau\hat{n} \tag{1}$$

where E is the bank erodability coefficient (L/T per unit stress); τ is the bank shear stress; and $\hat{n}$ is the unit vector perpendicular to the downstream direction (Table I).

The landscape in CHILD is represented by an adaptive irregular mesh of nodes. The advantage of this type of mesh is that nodes can be moved, added, or deleted to represent evolving geometries in a landscape. This capability is used here to simulate the gradual development of complex-shaped meander bends (Figure 1). During the meandering process, the central channel nodes are relocated, any obstructing outer bank nodes are deleted, and additional nodes are added behind the former channel position to create point bars (Figure 1; Lancaster, 1998). Because of channel movement, the floodplain mesh is continuously updated. Meander segments that approach one another are able to link to create neck cut-offs.

The bulk of the alluvial fill in many systems is not represented by the deposits of the meandering channel, but by fine-grained overbank sediments. CHILD therefore includes a module that simulates overbank deposition, using a modified form of Howard's (1992) floodplain diffusion model. This approach is based on the observation that floodplain sedimentation rate decreases exponentially with distance from the main channel due to turbulent diffusion of suspended sediment in flood waters (Pizzuto, 1987; Howard, 1992, 1996; Mackey and Bridge, 1995). The depth of aggradation at a point on the floodplain during a given flood event is:

$$dH_{overbank} = \mu(W_{chan} - Z_{fp}) \exp(-d/\lambda_{ob})\Delta t \tag{2}$$

where $dH_{overbank}$ is the depth of sediment deposited during a flood event at a floodplain node, μ is the near-bank deposition rate per unit flood depth (dimensions of $1/T$

Table I. Key constants from the channel hillslope integrated landscape model (CHILD) input file, and variables from the demographic equations.

Symbol	Explanation	Value	Equation
E	Uniform bank erodability	0.0005 m/Nyr	1
μ	Overbank deposition rate constant	0.25 m/kyr	2
λ_{ob}	Overbank distance-decay constant	750 m	2
K_h	Bankfull depth-discharge coefficient	0.028	3
m	Bankfull depth-discharge exponent	0.4	3
Q	Mean river discharge	~100 m³/s	3
STDUR, Δt	Mean storm and flood duration	0.06 yr	2
INSTDUR	Mean interstorm duration and geomorphic calculation time step size	1 yr	—
Δx	Initial Triangular Irregular Network (TIN) cell size	50 m	Fig 1.
R_{growth}	Population growth-rate constant	0.4	5
g	Generation, demographic calculation time step	15–30 yrs	5
K_i	Maximum population carrying capacity at settlement i	< ~2000	7, 8, 9
K_{max}	Maximum population carrying capacity floodplain (Note that equations are stochastic and, therefore, maximum values are > 2000)	2000	6
$X_{i,g}$	Population at settlement i during generation g	< 2000	7, 8, 9, 12
D_{max} & Ds_{max}	Maximum possible distance to another settlement (constant; diagonal model distant)	7071 m	6, 10
Dc_{max}	Maximum distance to the migrating channel (evaluated per generation for the model area)	~2500 m	10
L_s	Suitability of a floodplain location for settlement initiation		10
P_s	Probability of local settlement initiation		11

where T stands for time), λ_{ob} (dimension of length, L) is the distance-decay constant at which overbank sedimentation rate decreases to zero, and d (L) is the distance between a given point on the floodplain and the nearest point on the channel. At any point along the channel, flood depth, H_{chan}, and water-surface height, W_{chan} (= H_{chan} + Z_{chan}, where Z_{chan} is channel-bed height), are calculated using a standard rating curve:

$$H_{chan} = K_h Q^m \tag{3}$$

where Q is discharge (L^3/T) and Z_{chan} is the altitude of the channel bed. The flood depth at any point on the floodplain, H_{fp}, is calculated by subtracting the local topographic height, Z_{fp}, from the water-surface height at the nearest channel point:

$$H_{fp} = W_{chan} - Z_{fp} \tag{4}$$

Thus, the rate of overbank sedimentation at any point depends on topography and flood discharge. The latter is controlled by the sequence of storm events, in which event intensity (runoff and discharge) and duration (Δt) are drawn at random from exponential frequency distributions (Tucker and Bras, 2000).
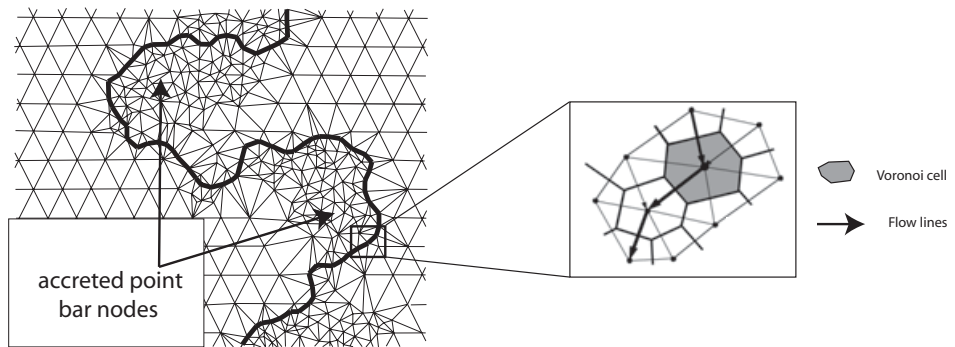
Figure 1. Planform example of river meandering simulated on a Delauney Triangulated mesh in the Channel Hillslope Integrated Landscape Model (CHILD). The mesh densification is the effect of the accretion of point bar nodes that trail the moving position of the channel.

Channel-Bed Elevation and Alluvial Deposition

The altitude and gradient of natural channels typically varies over time, in tune with fluctuations in the balance between sediment load and stream power (e.g., Bull, 1979). The ultimate controls on these oscillations, whether climatic, tectonic, eustatic, or other, usually extend well beyond the bounds of any individual valley segment. One strategy for modeling these oscillations in a valley segment would be to compute the river's response to varying water and sediment delivery upstream (e.g., Hancock and Anderson, 2002) and varying base level downstream (e.g., Snow and Slingerland, 1987; Clevis et al., 2004). The drawback to this approach is that it involves at least three poorly known independent variables. For this reason, we take the simpler approach of treating the river elevation itself as a boundary condition. The upstream and downstream ends of the river are driven upward or downward over time to represent externally imposed cycles of aggradation or incision. The total elevation drop between upstream and downstream is held constant. The river gradient is, therefore, equal to the upstream–downstream altitude difference divided by the total length of the channel. Because river length fluctuates through time as meander bends grow and are cut off, the river gradient also varies in time (but it does not vary in space). When a channel-bed point gains elevation, a layer of alluvium is added to the underlying sediment column, and when it loses elevation, the underlying sediment column is eroded.

Stratigraphy and Simulation of Deposition of Archaeological Features

A static rectangular grid that accumulates the subsurface stratigraphy underlies the irregular surface mesh representing the landscape topography. Each node in this grid contains a column of material divided into a series of stratigraphic layers of variable thickness and properties (Figure 2). Attributes of each layer include thickness, the relative proportions of alluvial sand and fine-grained overbank sediment, the time of
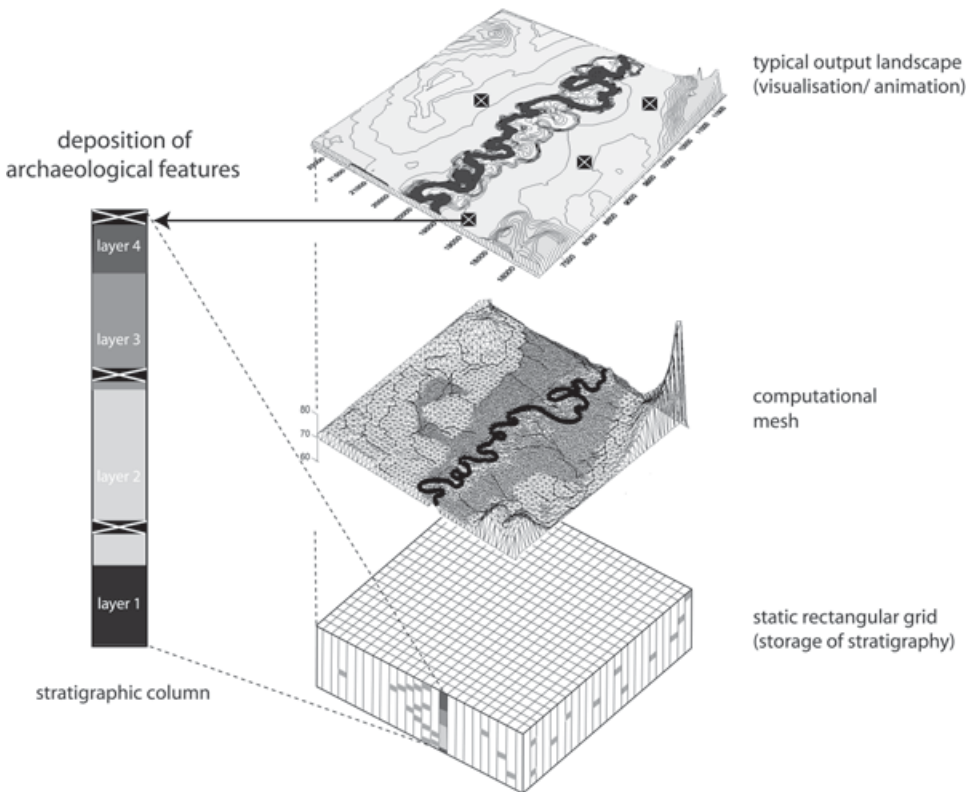
Figure 2. Overview of the meshes and methods used to simulate the meander floodplain landscape and its subsurface. Output landscape accentuated with topographic contour lines, historic positions of the meandering channel, and temporary settlement locations (top). Computational Delauney mesh used to dynamically move, add, and delete points in response to lateral movement along the channel (center). Static rectangular grid used for storage of the subsurface stratigraphy (below). The layers in the stratigraphic column store information on age, texture, and the density of buried archaeological features per cubic meter of floodplain sediment (left).

initial deposition, and the time the layer was most recently affected by erosion or deposition. In addition, each layer contains a "pointer" to surrounding layers as part of the linked-list data structure (Oualine, 1997), which is used to store the subsurface stratigraphy (Clevis et al., 2006). This data structure allows for dynamic memory allocation and, therefore, memory-efficient shrinking and growing of the layer stacks at specific grid locations as they are updated by surface erosion and deposition.

To explore the archaeological dimension, we also simulate the creation of sites. The generation of archaeological sites is modeled using a simple, time-invariant algorithm for settlement dynamics. At any given time, the valley segment will contain one or more individual settlements. During each generation of its existence, a settlement will generate "sites" within the surface sediment layer on which it rests.

In general, settlement initiation, growth, and relocation on an active floodplain are dependent on a multitude of factors. Here, we are interested simply in demonstrating the principle of coupled geomorphic-archaeological modeling, so we consider only a very limited subset of possible factors. These are discussed below. First, we note that the biggest simplification in the settlement model is the neglect of changes through time in land use and social organization. For example, we do not attempt to model a change in subsistence pattern from hunting and gathering to agriculture, nor do we deal with potential impacts of widespread deforestation. Such changes are undoubtedly important, and hypotheses regarding the nature of subsistence patterns or vegetation change could be studied using the methods we describe. In the present article, however, the aim is to present a proof-of-concept demonstration of the methods rather than to model the geoarcheaological evolution of any one particular place or time.

To illustrate an example of possible connections between behavior and the physical environment, we hypothesize that settlers will tend to prefer topographic high points, such as river terraces and natural levees, because these provide protection from river floods. Another factor included in the model is the preference for locations close to the river. This represents, in a very simple way, the importance of riverine resources, such as water, fish, and rich alluvial soils for cultivation and agriculture. As these are two contradictory motives, they are evaluated probabilistically (see Equations 10 and 11 below). Additional factors, such as sociodemographic characteristics of ancient societies, have been incorporated in advanced agent-based modeling studies (Dean et al., 2000; Kohler et al., 2000). In this study, we keep the "settlement rules" deliberately simple, but with a link to the morphology and flooding history of the alluvial valley. The flooding history is calculated in time increments that represent one flood and the succeeding interval before the next flood. Flood events vary in intensity and duration but occur approximately once a year. The archaeological simulation is divided into a number of generation calculation steps, each of which has a randomly determined time span between 15 and 30 years. The starting population for the model space is two inhabitants. During each generation, the number of inhabitants in the settlements is increased according to the Verhulst logistic population growth curve (Verhulst, 1838):

$$X_{i,g+1} = X_{i,g} + R_{growth}X_{i,g}\left[\frac{K_i - X_{i,g}}{K_i}\right] \tag{5}$$

where $X_{i,g+1}$ is the population of settlement i for a new generation $(g+1)$, R_{growth} is the rate of growth, and K_i the local settlement's population carrying capacity. K_i limits the local population growth and is a function of the competition with other villages:

$$K_i = K_{max} - \sum_{s=1,N_s}\left[1 - \frac{D_{s\to i}}{D_{max}}\right](X_s), \text{ for all } D_{s\to i} \leq D_{max} \tag{6}$$

This competition is expressed by decrementing a base value for carrying capacity (K_{max}) by the number of inhabitants (X_s) of neighboring settlements (N_s), weighted

by their relative distance (D_s) to the settlement i. The maximum possible distance of influence is D_{max} (here taken to be ~7 km).

Half of a settlement's population increase per generation is allowed to migrate to neighboring settlements or to pioneer a new settlement location. The probability of this happening during a generation is expressed as the ratio between the settlement's population and carrying capacity:

$$P_{migrate,i} = \frac{X_i}{K_i} \tag{7}$$

$$P_{pioneer,i} = \frac{1}{N_s}\left[\frac{X_i}{K_i}\right] \tag{8}$$

The probability of pioneering a new settlement takes into account the density of settlements in the area by weighting the probability with the number of existing settlements (N_s).

A settlement may attract migrants from another settlement, and the probability for doing so is determined by the difference between the current population and the carrying capacity:

$$P_{attract,i} = \frac{K_i - X_i}{\sum\limits_{s=1,N_s}(K_i - X_s)} \tag{9}$$

Selection of the new location is based on the suitability of the nodes in the simulation area, which is given by a selection function. The suitability for each cell in the model landscape to attract a group of settlers per generation is given by three factors: the generation-average depth of flooding, the distance to the riverine resources, and the distance to other, competing villages:

$$L_{select,i} = \left[\frac{W_i - Z_i}{H_{max,g}}\right]\left[\frac{Dc_{max} - Dc_i}{Dc_{max}}\right]\left[1 - \frac{Ds_{max} - Ds_i}{Ds_{max}}\right] \tag{10}$$

and

$$P_{select,i} = \frac{L_i}{\sum\limits_{1,N_s} L_s} \tag{11}$$

where the flood determinant is expressed as the ratio of the difference between local water height (W_i) and elevation (Z_i) to the maximum flood height in the simulation area (H_{max}) per generation. Obviously, inhabitants of natural floodplains are expected to have a memory for flood-risk areas and pass this information to future generations. This transfer of knowledge could be easily incorporated into Equation 10 by increasing the time span for which H_{max} is calculated. The relative proximity to the river is given by the ratio between actual distance (Dc_i) and the maximum distance to the channel (Dc_{max}). Similarly, the competition factor is determined by the ratio between the closest distance to another settlement (Ds_i), and the maximum possible distance to another settlement (Ds_{max}).

Settlements in the simulation are abandoned due to two processes. First, when a settlement is competing with a number of settlements close by, its carrying capacity is affected dynamically and may result in a population decrease (Equation 6). In this case, when the population approaches zero, the settlement is abandoned. Second, poorly chosen settlement locations can be flooded several times per generation in the model. The probability for abandonment in a given generation due to flooding risks is given by the formula:

$$P_{abandon,i} = \left[\frac{W_i - Z_i}{H_{max,g}} \right] \left[1 - \frac{X_i}{K_{max}} \right] \qquad (12)$$

where the first factor in parentheses is the relative local flood height as in Equation 10, and the second factor expresses the increased chance of survival for the larger settlements with a population (X_i) close to carrying capacity (K_{max}). The number of inhabitants controls the size of the settlements; every 250 m^2 cell in the model accommodates about 10 people. The L-shaped form of the settlements is an artifact of the algorithm that lets the settlements grow and shrink according to the continuously changing population.

All settlements generate a number of archaeological items at a fixed rate of 10 per capita. These items are buried by flood sedimentation and subsequently incorporated into the subsurface stratigraphy during activity and after abandonment of the settlement (Figure 2). The resulting density of the archaeological items in the subsurface is, therefore, a function of both the settlement dynamics and the local sedimentation rate. Stratigraphic horizons with a low sedimentation rate accumulate a high density of archaeological items due to their long surface-exposure history, whereas layers deposited under high sedimentation rates show a low density of items because of dilution.

As noted above, this settlement model is chosen for illustrative purposes and is obviously a highly simplified representation of archaeology. It neglects a host of factors, such as seasonal occupancy of hunter–gatherer sites, historic memory for floods, or differentiation in the type of archeological material buried in the subsurface. The settlement rules were chosen for two reasons: to demonstrate an explicit and plausible link between settlement behavior, archaeological sites, and the hydrogeomorphic environment; and to illustrate the potential for using this type of model to examine the archaeological (and potentially measurable) consequences of alternative hypotheses about human settlement behavior.

SCENARIOS AND RESULTS

Studies of Late Glacial and Holocene meandering river systems have shown that periods of floodplain aggradation and incision correlate, to varying degrees, with climatic proxies and land-use changes (Starkel, 1988; Vandenberghe, 1995; Mäckel et al., 2003; Macklin and Lewin, 2003). Periods of increased flood frequency, floodplain aggradation, and lateral river activity often result from phases of climatic cooling and higher rainfall, as indicated by corresponding glacier advances, tree-line retreats, and δ^{18}O records. Here, we simulate the development

of three river valleys by climatically controlled variations in discharge and aggradation rate that are representative for the Holocene. These scenarios are meant as templates for thinking about potential forms of valley evolution and visualizing the effect the evolution may have on the distribution of archaeological material in the subsurface. They are not intended to reconstruct any specific valley or archaeological field site.

The first scenario represents the simple case of steady channel and floodplain aggradation. The main channel aggrades at 1 m/1000 years over a 12,000-year period. This simple scenario serves as a comparative case for two more complex valley-evolution scenarios. In the second scenario, the channel elevation follows a more complex floodplain-elevation history based on that of the Pomme de Terre River in southern Missouri, as reconstructed from radiocarbon terrace dates by Brakenridge (1980). This floodplain history shows that periods of river stability are rare throughout the Holocene and that the valley evolution is dominated by millennial-scale cut-fill cycles with a maximum elevation difference between terraces and channel bed of 8 m.

In the last scenario, the history of channel aggradation and incision is varied according to the $\delta^{18}O$ curve for the Holocene (Schulz and Paul, 2002). Lows in the $\delta^{18}O$ value of this curve correlate with millennium-scale climatic deteriorations in Europe during the Holocene (Dahl and Nesje, 1996; Haas et al., 1998) and seem to correspond to periods of increased flooding, alluviation, and preservation of alluvial units in the British Isles, as indicated by studies of the relative abundance of available fluvial radiocarbon dates (Macklin and Lewin, 2003). This effect is introduced by using the trends in the $\delta^{18}O$ curve to steer the channel-bed aggradation history, with $\delta^{18}O$ decreases corresponding to aggradation and $\delta^{18}O$ increases to incision. In doing so, we assume that there is no time lag involved in the climatic steering and the geomorphic response of the aggrading channel bed (Hancock and Anderson, 2002). The overall aggradation simulated is 4.5 m, a value that approximates the cumulative sediment thickness for a small Holocene lowland river (Törnqvist et al., 2000).

Scenario 1: Steady Aggradation

Valley evolution in the steady aggradation scenario is shown in time steps of 1200 years in Figure 3. The simulation starts with an initial straight channel superposed upon a digital terrain model of a floodplain at 10,000 B.C. Minor irregularities in the initial channel pattern evolve to a set of meander bends by 7600 B.C., at which point they are on the verge of cutting off (Figure 3c). At 5200 B.C., the outline of the main channel belt is delineated by a suite of abandoned meander loops flanking the active channel, while the surrounding floodplain is gradually buried by overbank deposition and forms a slightly convex-upward topography in cross-section (Figure 3d). Settlements tend to relocate on a time scale smaller than the landscape snapshots shown. However, the larger settlements developed on the higher levee positions flanking the channel are less flood-prone, and, therefore, tend to remain active for time spans of a few hundred years. The settlement model
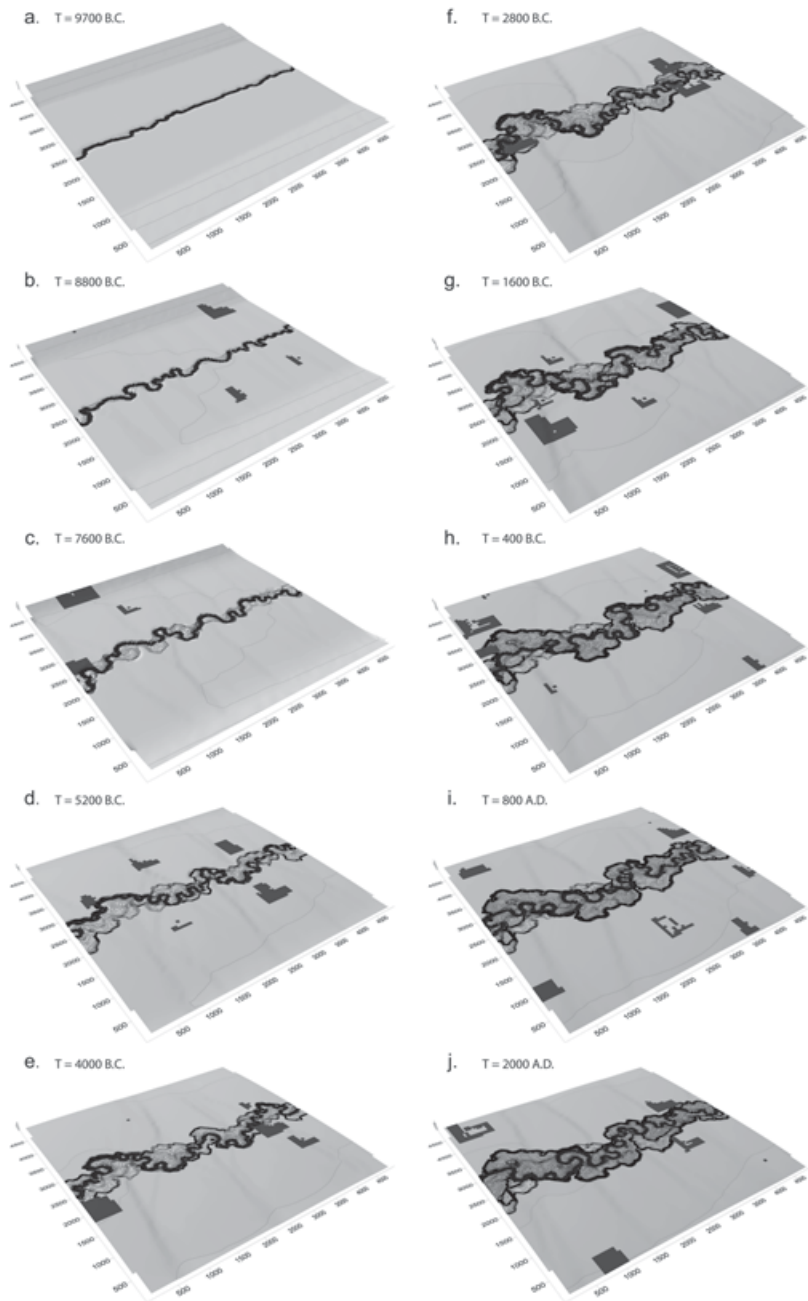
Figure 3. Perspective views showing the development of the simulated meander floodplain landscape during steady aggradation (Scenario 1). Active settlement locations are indicated in black. The shaded linear features perpendicular to the channel belt are undulations caused by increased rate of sedimentation on the floodplains due to the changing position of the nearby river bends (~sediment sources).

applied is very simple, as it is not specific to any historic period and it does not take into account regional population variation, technological development, or sociocultural change. Nonetheless, the example in Figure 3 does serve to demonstrate how the hypotheses used in this type of coupled model yield potentially testable outcomes: in this case, a prediction about the mean and frequency distribution of settlement occupation durations.

Settlements show phases of initiation, growth, decline, and sometimes reoccupation (as can be seen, for example, in Figure 3d–f and j at coordinates $x = 3500$, $y = 3500$). Smaller settlements pioneering the more flood-prone positions on the floodplain are relatively short-lived and tend to disappear within 100 years. During the scenario, fine-grained overbank sediment is continuously deposited in the simulation area by incremental small flood events. Consequently, any archaeological features related to the settlements become incorporated into the accumulating floodplain and are eventually covered with sediment after abandonment of the settlement. The resulting 3D distribution of archaeological features in the floodplain subsurface at time interval A.D. 2000 is shown in Figure 4a. In this subsurface view, the floodplain sediments themselves are omitted and only the position and density of archaeological features is visualized (blue-green), together with the stack of sands deposited by the meandering channel (orange). The main cluster of larger archaeological features is positioned close to the channel belt stack, demonstrating the preference for settlement initiation and increased survival potential at the high levee locations. The archaeological features have a uniform density of about 0.25–0.5 per m³ of sediment because of the steady aggradation rate on the floodplain throughout the simulation. This steady aggradation rate is also reflected in the equal spacing of timelines in the floodplain cross-sections (white lines, Figure 4b, c). An increased archaeological site density, however, is observed in the lower-right corner of Figure 4a, where the settlement spreads upward onto a steep sloping terrace. Because floods are rare on this slope (due to its altitude), the rate of site burial is also low and, therefore, the site density is higher here than in the lower, more flood-prone portion of the settlement.

The channel aggradation trend is depicted in Figure 5a, together with the development of the channel sinuosity, both indicating a steady development of the geomorphic system. The historical population activity on the simulated floodplain is given in Figure 5b. This curve reaches its average maximum value of 3000 inhabitants in about 1500 years but then takes the shape of a saw-tooth, where gradual population increases are punctuated by rapid declines, once every 200–500 years. These phases of decline in the population correspond to major flooding events triggered by the storm simulator, resulting in flood depths large enough to increase the chance of abandonment of multiple settlements (Equation 12). Besides modification of the active settlement pattern by flooding events, lateral channel migration also affects settlements close to the channel. Both active settlements and abandoned settlements hidden in the subsurface are lost due to erosion by lateral channel migration. This effect becomes increasingly important through time as the channel belt widens and populated levees are eroded together with settlements buried in the reach of the channel base (Figure 5c). Consequently, the shape of the curve describing the cumulative preserved archaeology in the floodplain subsurface is similar to the historical
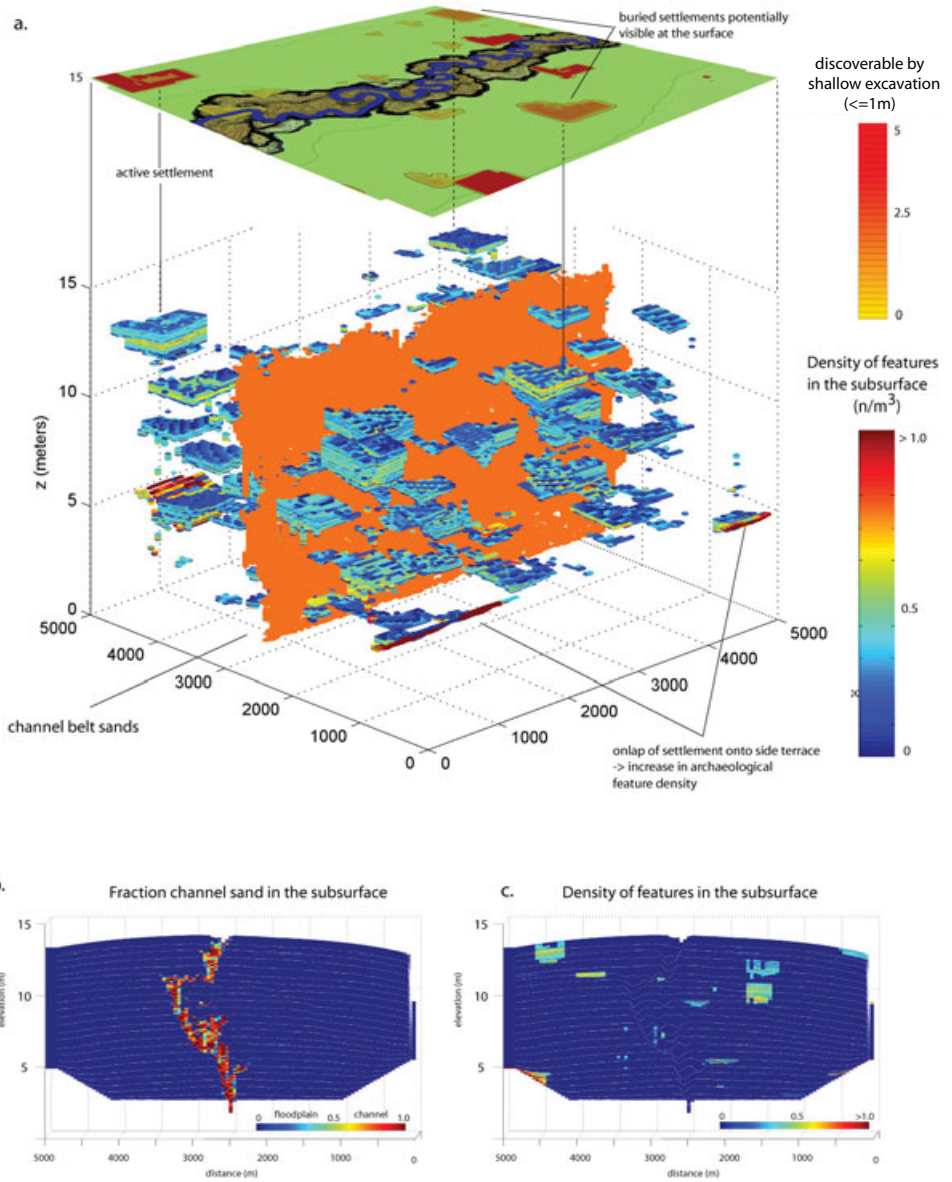
Figure 4. (a) Diagram showing the three-dimensional distribution and density of archaeological features in the subsurface of the floodplain (blue-green). The paleoposition of the channel is given by the stack of channel belt sands (orange). The surface landscape is annotated with a density contour map of the settlements buried in the shallow subsurface, which may be visible at the surface. (b) Stratigraphic cross-section through the floodplain showing the fraction of sand in the subsurface, delineating the position of the buried channel belt (red), and the floodplain sediments (blue). Equally spaced timelines each represent 500 years of steady floodplain aggradation. (c) Density of buried archaeological features.
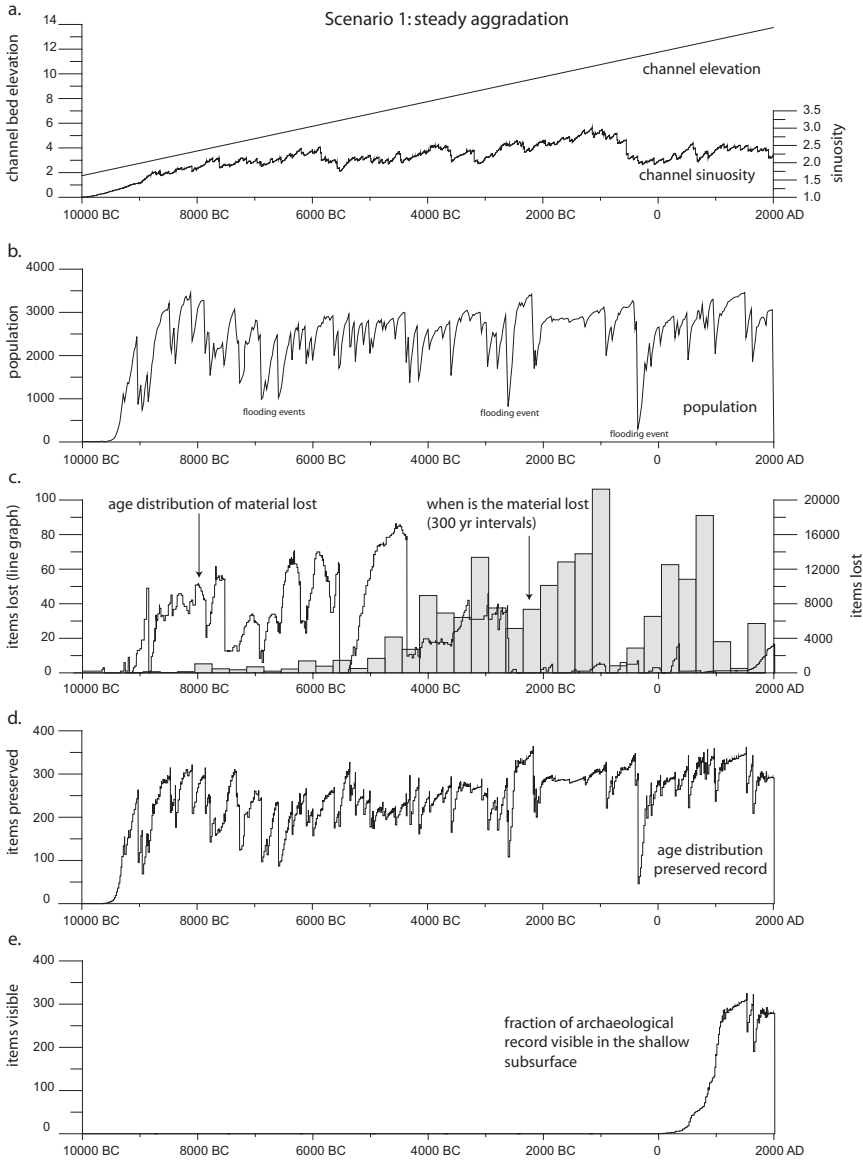
Figure 5. Graphs illustrating the historical coupling between geomorphic processes, population dynamics, and preserved archaeology in the subsurface for Scenario 1. (a) Channel bed elevation and channel sinuosity. (b) Floodplain population as a function of time. (c) Bar graph of the intensity of loss of archaeology in the channel per 300 years. Line graph of the age distribution of archaeology lost. (d) Age distribution of preserved archaeology present in the floodplain subsurface at 2000 A.D. (e) Age distribution of archaeology potentially exposed at the surface.

population curve, but with some minor truncations at around 8500–5000 B.C. (Figure 5d vs. 5b). The main demographic events (such as the population declines at 7000 B.C., 2800 B.C., and 300 B.C.) are well recognizable.

Again, we note that this population curve is in no way meant to represent any particular time or location; such a curve would be quite unrealistic for, say, northwestern Europe, where population increases toward later prehistory. Rather, the take-home message is that, under conditions of steady river sedimentation, there is little or no systematic bias introduced into the archaeological record by geomorphic activity (in particular, by stream erosion) in this scenario. Therefore, if one could obtain a good sample of the archaeological record throughout the subsurface, that sample would (all else being equal) provide a reasonably accurate picture of the actual population dynamics. However, most archaeological prospecting methods rely on the information present in the shallow subsurface, such as crop marks and features visible by means of geophysical survey techniques. To mimic this limited scope, the yellow colors on the surface in Figure 4a show only those settlements that are present in the top 1 m of the floodplain stratigraphy. Comparing the near-surface and subsurface view clearly demonstrates that most of the archaeology is hidden as a result of the steady aggradation, providing common archaeological surveying methods a time window of only ~2000 years in this example (Figure 5e).

Scenario 2: Aggradation Alternating With Incision

In the second scenario, the channel-floodplain system was subjected to a sequence of cut-fill cycles in which the amplitude and timing of the incision and aggradation phases was based on the channel history reconstructed for the Pomme de Terre River by Brakenridge (1980). The first quarter of meander evolution is similar to that of Scenario 1, in which the channel belt widens (Figure 6a–c until 6000 B.C.). Different from Scenario 1 are the phases of incision clearly visible in Figure 6f, h, and i. The abandoned and incised meander bends become filled by fine-grained sediment during subsequent phases of aggradation (Figure 6d, e at 5200–4000 B.C., and j at 2000 A.D.). The cut-fill cycles of the channel leave a clear imprint on the stratigraphy of the floodplain (Figure 7). The initial phase of steady aggradation (10,000–6200 B.C.) created the bulk of the stratigraphic volume, characterized by equally spaced timelines visible in the cross-sections (Figure 7). The first incision event at 6200 B.C. corresponds to the hiatus marked by the superposition of two timelines at ~8–10 m altitude (Figures 7b–f). During 5800–3500 B.C., the channel then aggrades from a position incised into the floodplain to a level at which it can flood the valley again and deposit sediment in the surrounding floodplain. None of the subsequent aggradation phases reaches a higher elevation, and the 5800–3500 B.C. alluvial sequence dominates the floodplain as a terrace. The cut-fill cycles postdating the 3500 B.C. terrace occur within the incised channel belt but result in a complex superposition of depositional ages, which varies per cross-section due to the 3D effect of meandering (Figure 7b–d). The cut-fill cycles also affect the distribution and density of archaeological features in the floodplain. The larger features in the subsurface are synchronous with the initial phase of aggradation (Figure 7a, below 10 m) and are positioned close to the chan-
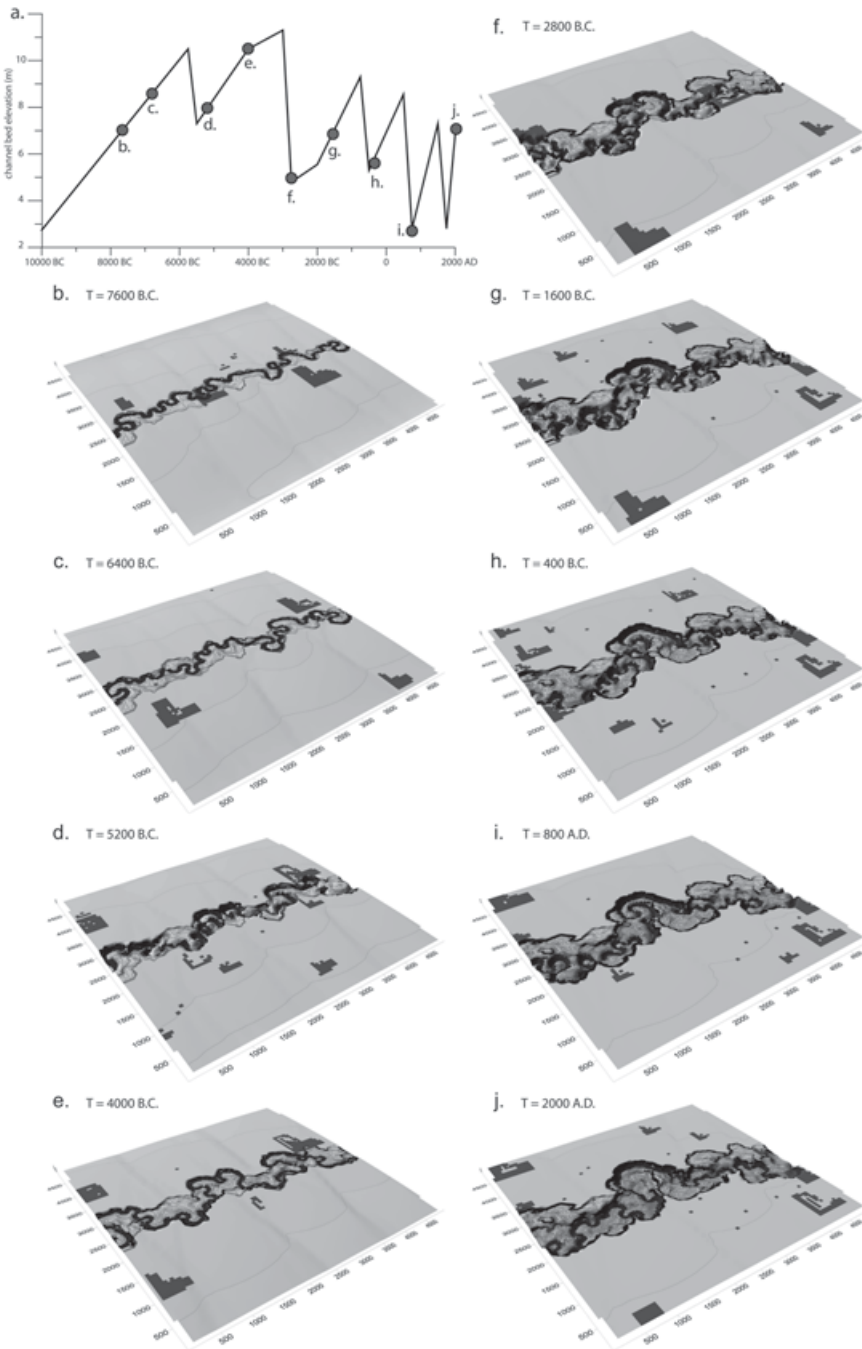
Figure 6. Perspective views of the meander floodplain landscape evolution dominated by alternating phases of aggradation and incision (Scenario 2). Active settlement locations are indicated in black.
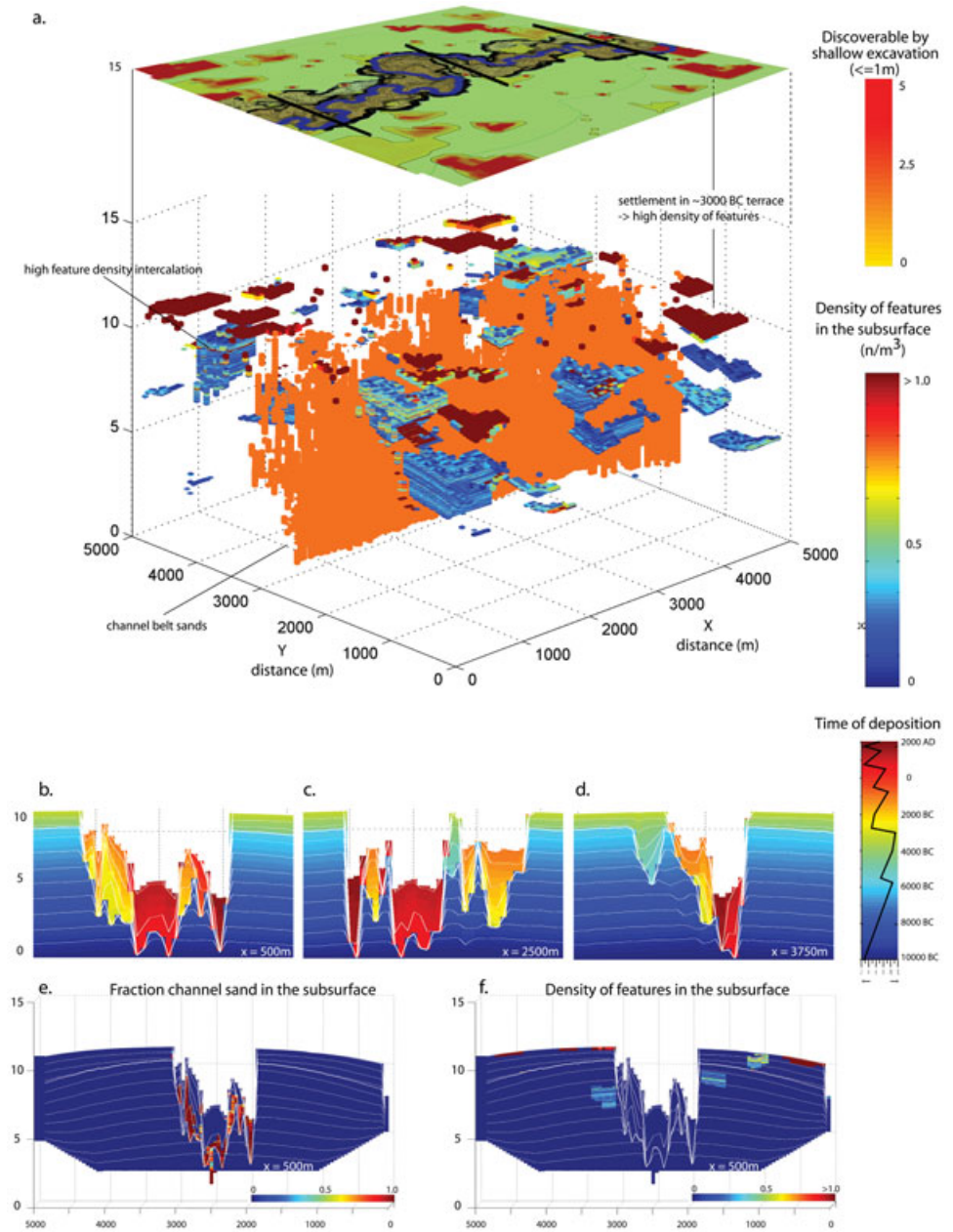
Figure 7. (a) Three-dimensional distribution of archaeology in the floodplain resulting from the cut-fill Scenario 2, showing high-density features in the top of the stratigraphy corresponding with a terrace level. (b–d) Cross-sections of the alluvial stratigraphy colored according to the time of deposition. (e and f) Cross-sections showing the channel sands and the density of buried archaeological features.

nel belt, whereas settlements corresponding to the incision at 6000 B.C. and the second half of the simulation (above, from 3000 B.C. onwards) are distributed more equally through the stratigraphic volume. These phases correspond to decreases in the number of valleywide flooding events, increasing the chance of survival of settlements positioned at low locations on the floodplain. Furthermore, in contrast to Scenario 1, the number and density of archaeological features at the surface and in the shallow subsurface is much higher, especially in the 3500 B.C. terrace. This is because the terrace is exposed continuously during the second half of the simulation time, accumulating most post-3500 B.C. archaeological features in its stratigraphy. The settlement buried in the terrace at $x = 4500$, $y = 750$ (Figures 6f–j, and 7a), for example, shows a high density of features. Some buried settlements even contain a high-density level intercalated between intermediate density sediments ($x = 500$, $y = 4000$) at 3500 B.C. This change in density results solely from the geomorphic system (as noted above, no attempt has been made to make settlement behavior period dependent), and it illustrates one way in which a geomorphic phenomenon could be misinterpreted as a cultural one.

The historical population curve is similar to that of Scenario 1, showing an average of 3000 inhabitants, although there are two interesting differences (Figure 8b vs. Figure 5b). As in Scenario 1, the first segment of the curve (10,000–3500 B.C.) is dominated by multiple small declines in the population, but the second segment is less noisy and only shows occasional large declines in the population. Most of these large declines correlate with the phases of aggradation.

The pattern is explained by the effect the cut-fill cycles have on the flood frequency in the floodplain. In the period after 3500 B.C. most settlements are spared from abandonment by flooding and because of their position on the terrace, well above the channel bed. Only during the aggradation phases (~800 B.C. and 200 A.D.) are the flood depths large enough to increase the chance of abandonment of multiple settlements. The loss of archaeological features in the subsurface begins during phases of incision (5800 B.C., 3000 B.C., and 500 A.D.). Again, the curve for the preserved archaeological record (Figure 8d) is a reflection of the population history minus the loss in the channel belt, with clear truncations at 7500 and 3000 B.C. The fraction of the record visible in shallow subsurface is much larger due to the continuous exposure of the 3500 B.C. terrace (Figure 8e).

Scenario 3: Aggradation Alternating with Incision, Δo^{18}-Curve

The Holocene $\delta^{18}O$ curve (Schulz and Paul, 2002) drives the cut-fill cycles in Scenario 3. The $\delta^{18}O$ decreases are assumed to correspond to aggradation (increasingly cold periods typically correlated with alluviation in northern Europe; Macklin and Lewin, 2003) and $\delta^{18}O$ increases to incision. This scenario is more complex than the previous two because the channel is affected by four major phases of alluviation (8000 B.C., 6500 B.C., 2500 B.C., and 2000 A.D.), alternating with multiple small aggradation-incision cycles (Figure 9a, d–h). The resulting alluvial stratigraphy is equally complex (Figure 10a), showing composite-age channel belt sands embedded in a floodplain with a discontinuous chronology. The chronology of the sediments in the channel
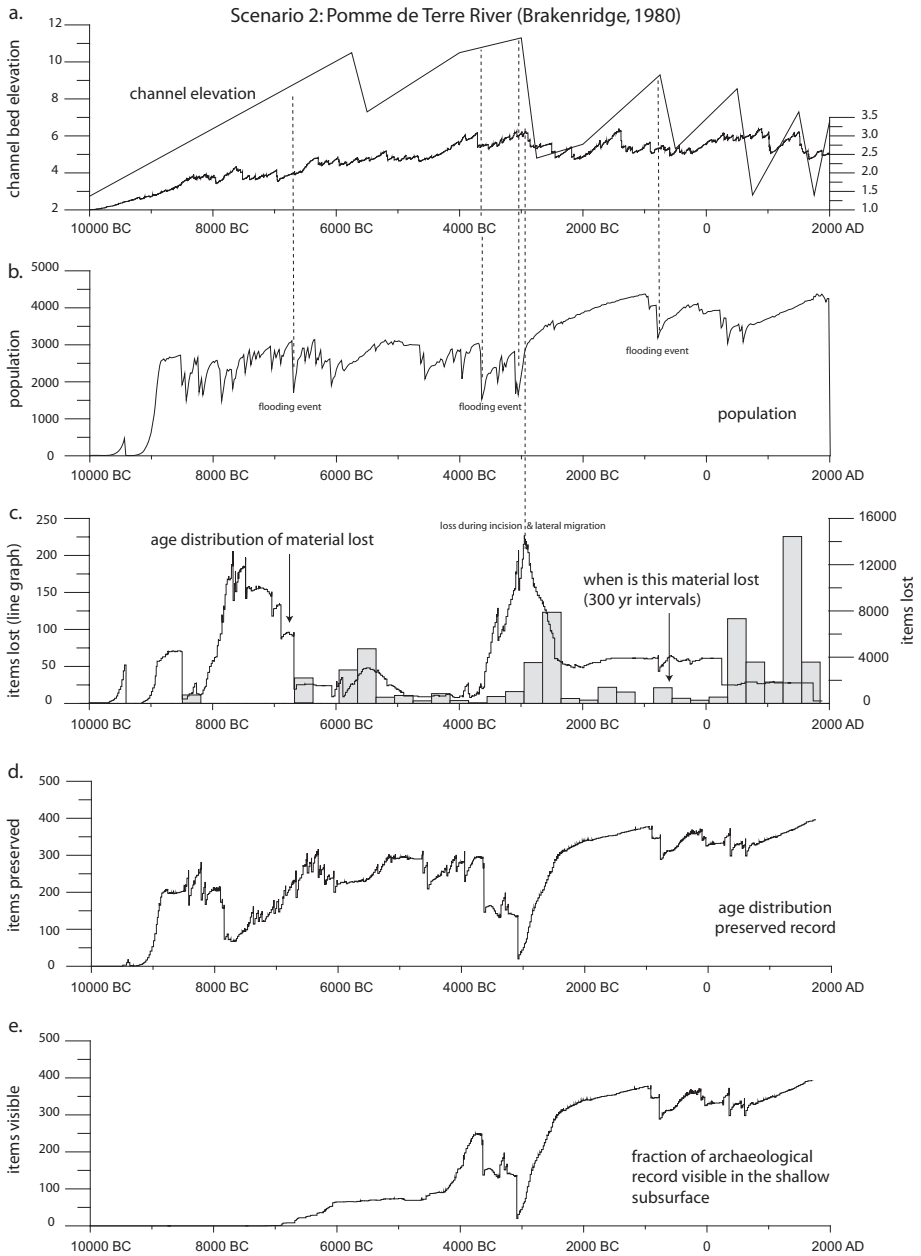
Figure 8. Graphs illustrating the historical coupling between geomorphic processes, population dynamics, and preserved archaeology in the subsurface for Scenario 2. (a) Channel bed elevation and channel sinuosity. (b) Floodplain population as a function of time. (c) Bar graph of the intensity of loss of archaeology in the channel per 300 years. Line graph of the age distribution of archaeology lost. (d) Age distribution of preserved archaeology present in the floodplain subsurface at 2000 A.D. (e) Age distribution of archaeology potentially exposed at the surface.
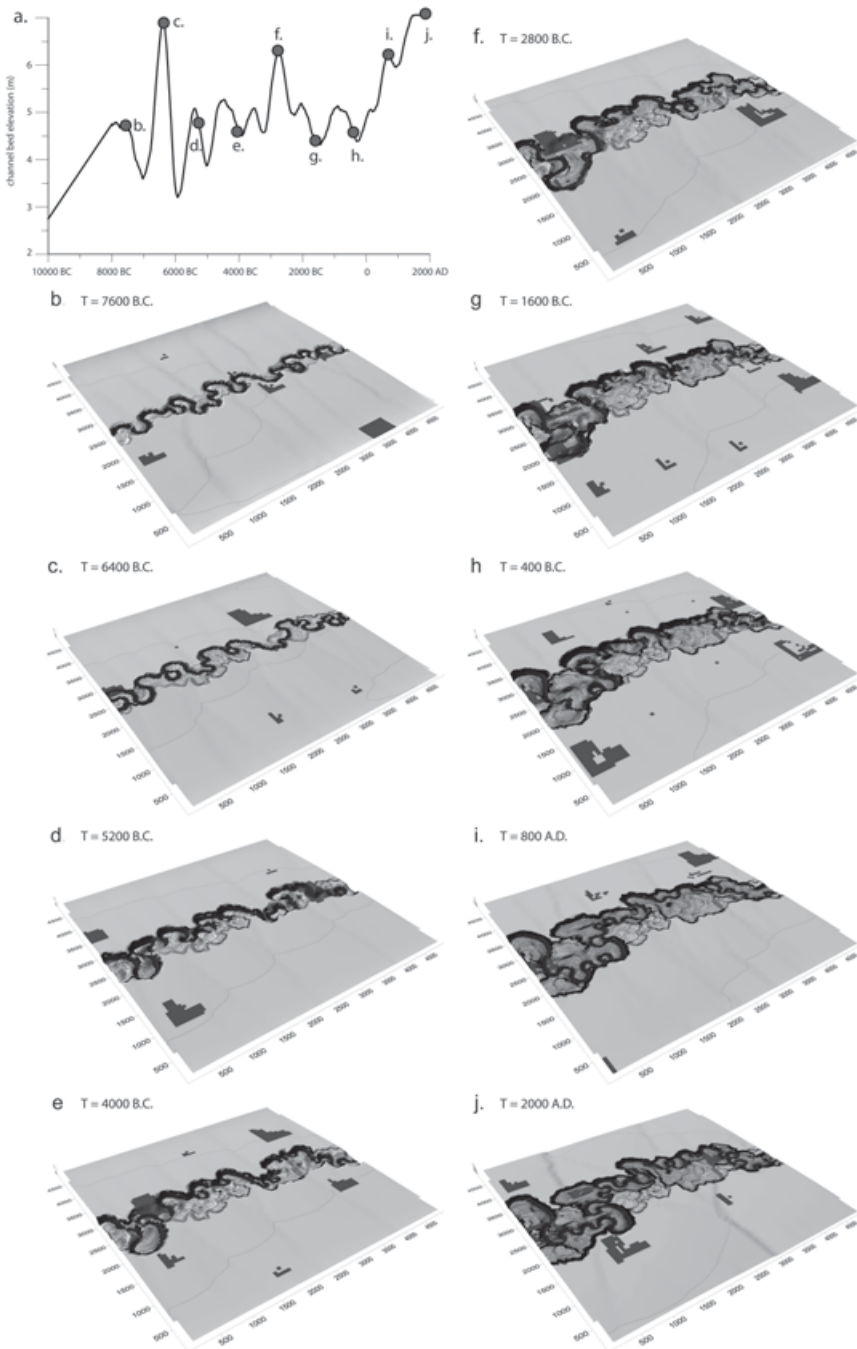
Figure 9. Perspective views of the meander floodplain landscape evolution dominated by alternating phases of aggradation and incision (Scenario 3). Active settlement locations are indicated in black.
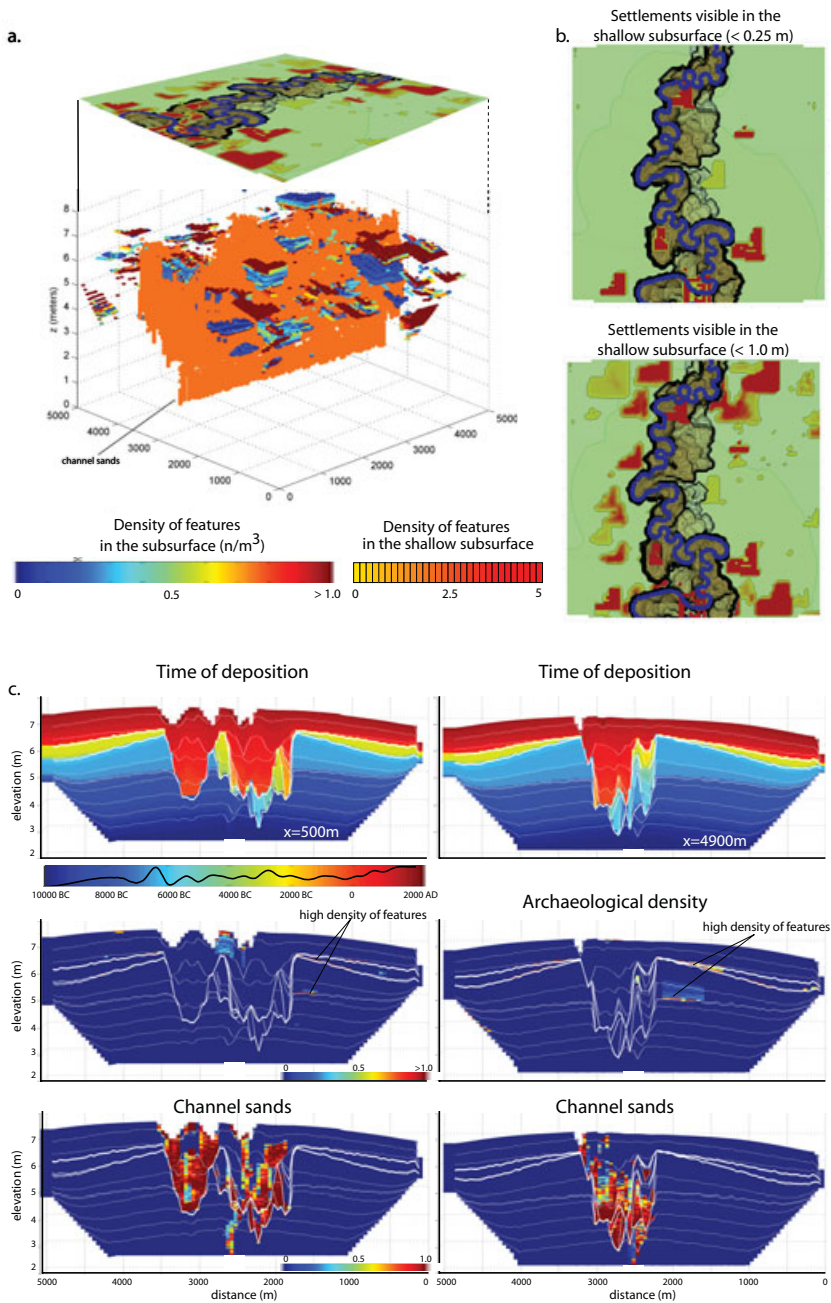
Figure 10. Three-dimensional distribution of archaeology in the floodplain resulting from the cut-fill scenario 3, showing a high density of features in the top of the stratigraphy corresponding with a terrace level. (b–d) Cross-sections of the alluvial stratigraphy colored according to the time of deposition. (e and f) Cross-sections showing the channel sands and the density of buried archaeological features.

belt is relatively continuous and occasionally forms a lateral accretion-like pattern in the timelines when the channel moves (Figure 10c, right). The basal sediments of the floodplain correspond to the first phase of aggradation (Figure 10c, 10,000–8000 B.C., dark blue color below 5 m) and are overlain by a condensed sequence (i.e., a deposit representing an unusually long period of time, reflecting a low sedimentation rate). This condensed sequence is synchronous with the first phase of incision, during which the entrenched river is less likely to flood the valley and the alluviation rate on the surrounding floodplain, therefore, decreases. The second floodplain unit is deposited during the second rise in the channel bed during 7000–6500 B.C. The unit is incised at 6000 B.C., forming a terrace (Figure 10c, light blue below 6–6.5 m). This terrace is exposed for most of the simulation time but is flooded around 2500 B.C. (Figure 9f), resulting in a thin veneer of spatially discontinuous sediments tapering the central channel belt. The youngest unit representing the top 0.25–0.5 m of the floodplain stratigraphy is deposited during the last rise of the channel bed (1000–2000 A.D.) and covers the complete floodplain, including the 6000 B.C. terrace (Figure 10c, red unit). As in Scenario 1, the cut-fill cycles control the density of buried archaeological features. Two high-density horizons are generated by the cycles in Scenario 3: the condensed sequence at 5 m (8000 B.C.) and the intercalated horizon forming the top of the buried terrace. The terrace is relatively rich in archaeological features, but because it is buried the archaeological information is potentially hidden from surface observation (Figures 10a, b and 11e).

DISCUSSION

Visibility of Archaeological Features

The simulations demonstrate that the visibility and density of archaeological features at depth depends largely on the 3D spatial distribution and ages of the sediments deposited during habitation. In a valley that has experienced steady aggradation, the preserved subsurface record in a wide floodplain is likely to provide a representative sample of the settlement history, all else being equal. In addition, the density of archaeological features per cubic meter of occupied floodplain sediment is relatively uniform due to the continuous creation of archaeological sites within floodplain sediment. However, steady aggradation also tends to hide older features. The time window of archaeological observation is primarily a function of the floodplain aggradation rate and the depth of shallow-surface prospecting techniques.

Valleys that have undergone geologically recent cut-fill cycles provide a larger time window for archaeological observation. Condensed sections and terraces tend to accumulate more archaeological features because of their reduced sedimentation rates and long exposure histories, respectively. Continuous habitation on stable terrace surfaces increases the density of features and generates a palimpsest of settlement activity with a wide age range. However, these relatively rich units may be hidden in the subsurface by a later phase of alluviation. This effect might be expected for many small river systems in Western Europe because of anthropogenic influence on the landscape. More-efficient Roman and post-Roman land-use techniques caused
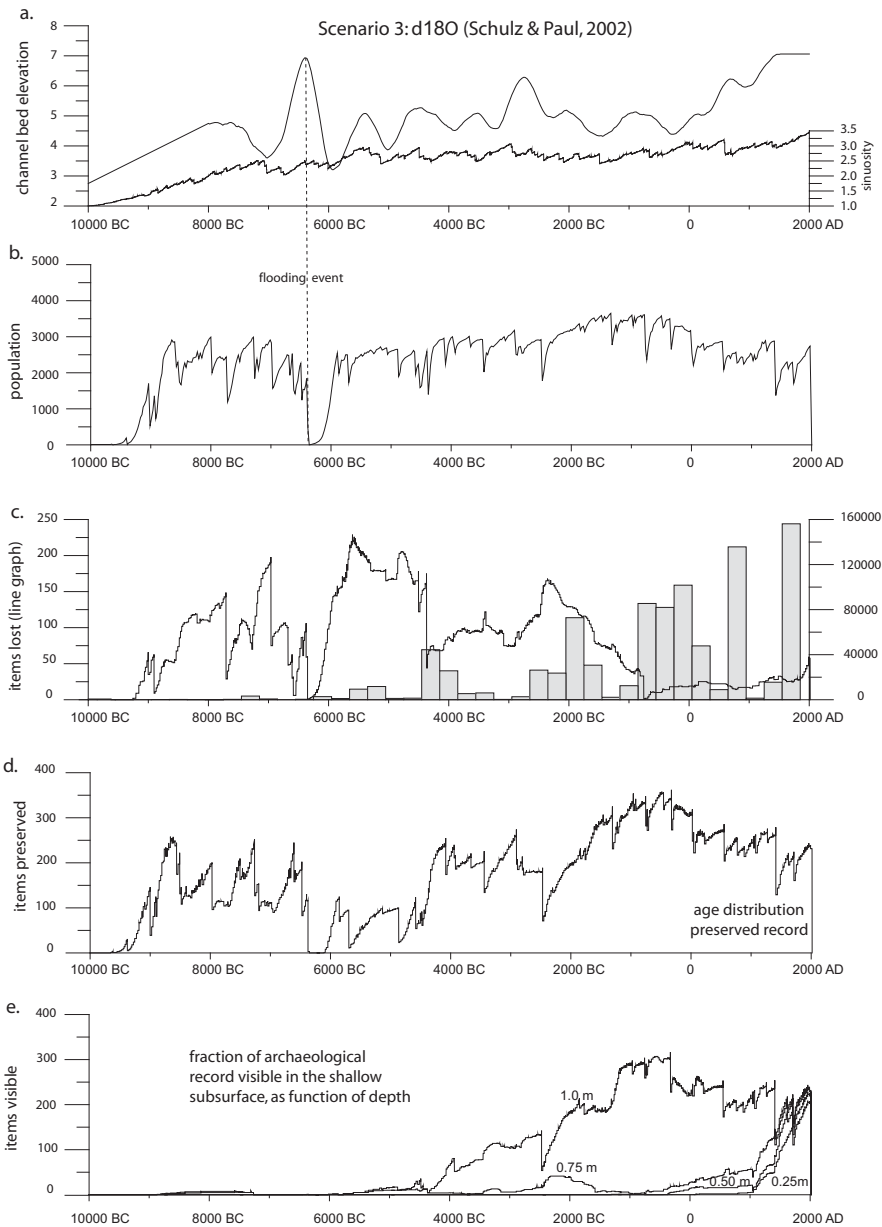
Figure 11. Graphs illustrating the historical coupling between geomorphic processes, population dynamics, and preserved archaeology at the surface for Scenario 3. (a) Channel bed elevation and channel sinuosity. (b) Floodplain population as a function of time. (c) Bar graph of the intensity of loss of archaeology in the channel per 300 years. Line graph of the age distribution of archaeology lost. (d) Age distribution of preserved archaeology present in the floodplain subsurface at 2000 A.D. (e) The age distribution of archaeology exposed at the direct surface differentiates from a shallow subsurface view, which includes the high-density buried terrace unit.

widespread hill slope erosion, higher sediment flux to rivers, and increased alluviation (Mäckel et al., 2003; Macklin and Lewin, 2003). Hypotheses regarding such changes in land use over time could be explored using the methods described here by constructing and running alternative scenarios and examining their implications for measurable archaeological and geomorphological patterns.

Preservation of Archaeological Features: The Effect of Floodplain Width

Besides visualizing the differential density of preserved archaeological material in the subsurface, the model also allows for quantification of loss of material due to erosion by lateral channel migration. The rate of loss is highest during phases of reduced aggradation or incision when the channel is able to expose and erode the archaeology buried in the channel banks. The cumulative loss of archaeological material in each scenario is summarized in Figure 12. The graph was generated by calculating the ratio between features lost by channel erosion and all features buried during a simulation. A floodplain-wide loss of 20% to 30% of archaeological information is observed for Scenarios 2 and 3, because they are dominated by cut-fill cycles (Figure 12, right). The terraces and condensed sequences in those two scenarios may accumulate an increased density of archaeological material, but this information is vulnerable throughout the long surface-exposure time of the units. Moreover, the high-density units are also affected by erosion after burial due to the shallow depth of burial within the reach of the channel bed.

A calculation of the loss for an increasingly narrow zone flanking the channel belt is used to demonstrate the effect of floodplain size (expressed as the ratio between floodplain and channel belt width) on preservation. The width ratio reflects the degree of floodplain recycling by the migrating channel. Based on this graph, it is expected that lowland rivers with wide floodplains, such as the Thames or the Rhine-Meuse, preserve most of the archaeological record. Small upland valley systems in contrast, could lose 45% or more of their archaeological record. Their zone of aggradation and preservation (e.g., the floodplain) overlaps with a large part of the channel belt, increasing the potential for erosion. An example of such a system is Wildcat Creek, Kansas (Johnson, 1999), where the floodplain is restricted by being encased between bedrock valley walls.

Evaluation of Excavation Schemes

The simulation modeling presented by itself cannot provide a means of precisely reconstructing any sediment horizon in the field due to the stochastic nature of the processes involved. Such reconstruction is never possible without prohibitively expensive and exhaustive ground proofing. What process-based simulation does provide is a virtual archaeological laboratory that can generate synthetic geoarchaeological data sets based on a user-defined geologic history. These data sets can be used to refine subsurface geostatistics or to test alternative survey and excavation schemes in a low-cost, nondestructive fashion. Figure 13 is an example of such an approach. In this example, five different sampling schemes are tested on the final land-
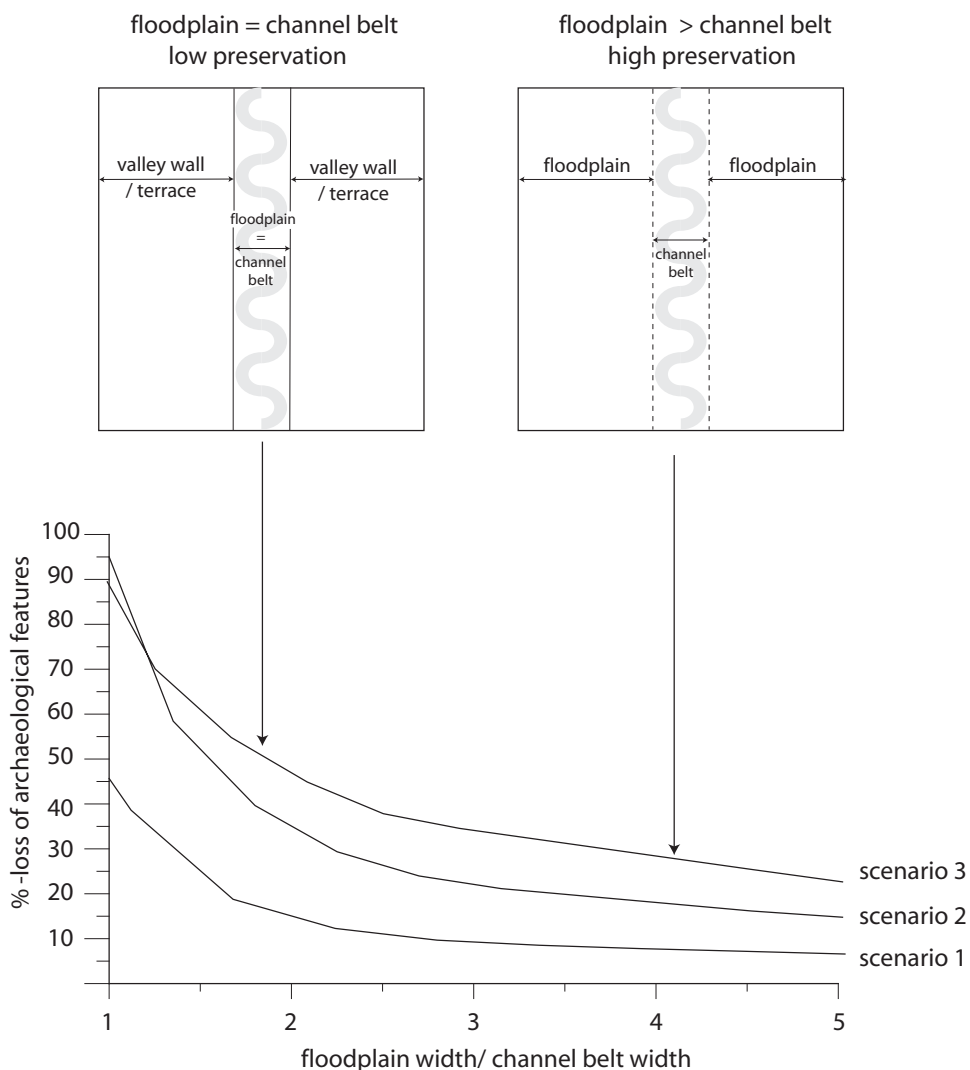
Figure 12. Plot of the percentage of loss of the archaeological record as a function of fluvial system size (expressed as ratio between floodplain and channel width). Based on the graph, it is expected that systems with small, upland floodplains encased by valley walls can lose up to 90% of their archaeological record, whereas in wide, lowland systems, most of the record is preserved.

scape of Scenario 2. The first scheme does not use any knowledge of the geomorphic or settlement history. Twenty-five pits, each 2 m deep and 1 m^2 in area, are sampled on a regular grid. The second scheme focuses on the locations with a relatively high density of archaeological features in the shallow subsurface, perhaps identified in an initial phase through aerial photography and geophysical surveys. The three other
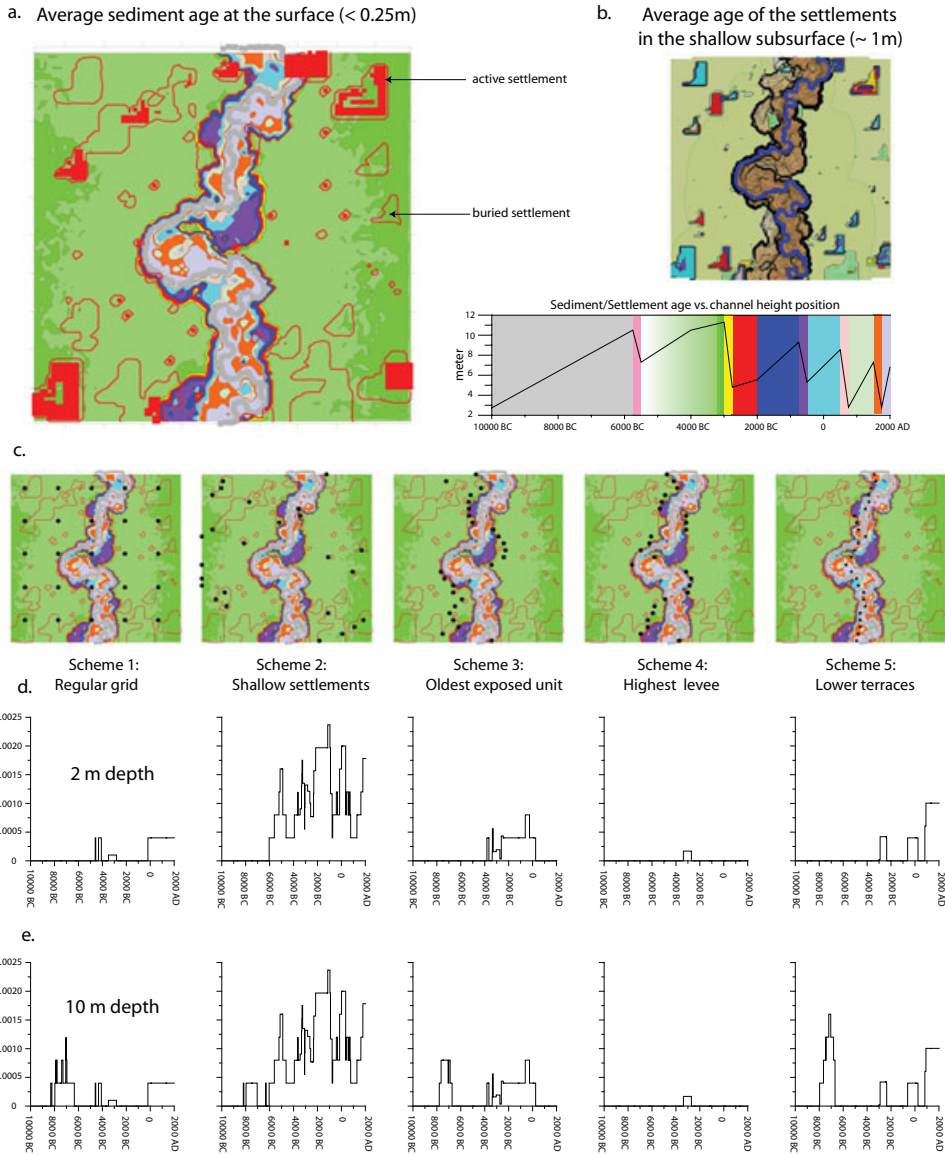
Figure 13. (a) Average depositional age of the sediments at the surface for Scenario 2 showing the dominant ~3500 B.C. terrace. (b) Palimpsest-like distribution of activity ages of settlements preserved in the shallow subsurface (depth < 1.0 m). (c) Excavation schemes used in the sampling of the floodplain subsurface. (d) Age distribution of archaeology recovered for excavation depths of 2 m, and (e) 10 m.

schemes are guided by geomorphic information, such as the presence of the oldest exposed unit (scheme 3), the center of the channel belt (scheme 4), and the highest levee positions (scheme 5). All five schemes are repeated for a sampling depth of 10

m (admittedly, this is unlikely for pits 1 m square, but in fact, for this exercise the absolute surface dimension of the excavation is unimportant; what matters is the relative differences between sampling schemes). The number of archaeological features and sites encountered is highest for the scheme guided by the shallow archeology, although the age distribution is highly skewed for both sampling depths, and the age distribution does not reflect the population curve (Figure 8b). The results for the oldest unit scheme are similar to that of the regular grid, mainly because the landscape is dominated by the 3500 B.C. terrace. In this case, however, older features are better represented. Both the schemes sampling the channel belt recover much less, as this zone is prone to flooding and less suited for settlements (scheme 4), and because the record is fragmentary due to loss by lateral channel migration. Ultimately, excavation schemes such as these could be tested and refined using simulated subsurface data sets that incorporate and honor both stratigraphic and archaeological information from the field. Added information might include preferential settlement locations, paleochannel positions, and subsurface geometries of pronounced flooding horizons.

In many valley systems, buried archaeological sites are threatened by sand-gravel aggregate mining (Kerr, 2004). The model presented here could be used to improve the recovery of such sites prior to aggregate extraction, by studying geomorphic controls on the spatial correlation between sand-gravel deposits and areas of archaeological concentration. One approach would be to use field data to constrain the late Quaternary geomorphic history of a particular valley system. This information would then be used to develop synthetic realizations that honor the available data, and provide a test bed for alternative survey and excavation strategies. This type of conditional simulation approach would restrict the number of possible scenarios for the sites being investigated and increase their predictive value by fitting the synthetic data to observational data in an automated process of trial and error (Cross and Lessenger, 1999; Bornholdt et al., 1999; Karssenberg et al., 2001).

The focus of this study has been to visualize and quantify relationships between fluvial architecture and archaeological subsurface resource distribution in a holistic fashion for increasingly complex geomorphic scenarios to illustrate the capabilities of the simulation approach. The model presented can be used as a tool to help archaeologists and cultural resource managers to visualize and interpret observed subsurface and surface patterns and develop an improved understanding of potential sources of geomorphic bias. However, the simulation approach also allows for systematic controlled experiments with a focus on a specific problem or a single variable. For example, one could test the ability of radiocarbon dating schemes with a limited number of samples to deduce floodplain history accurately for an assumed geologic scenario, estimating the kind of coverage (e.g., sample distribution and depth) that would be required or is most cost-effective. Alternatively, a set of experiments could be generated that examine whether, and to what degree, settlement preferences (such as proximity to water, protection from flooding, and defense) would produce diagnostic signatures in the alluvial archaeological record.

CONCLUSION

This study shows the potential of computer simulation in the characterization of alluvial valleys from a geoarchaeological perspective by providing a complete 3D subsurface view driven by a user-defined geomorphic history. Simulated fluvial systems that aggrade under steady rate are associated with a relatively uniform density of well-preserved archaeological features in the floodplain subsurface. Systems affected by cycles of entrenchment and alluviation form condensed sequences and terraces containing a high density of archaeological features but have the potential to lose a larger fraction of the archaeological record. The percentage of loss of the archaeological record by channel erosion depends on the frequency, depth, and duration of incision episodes and on the ratio of channel belt width to valley width. In the scenarios we have examined, predicted archaeological loss ranges from 45% or more for channel belt–dominated systems, decreasing exponentially to 10% for rivers where the floodplain width is a multiple of channel belt width. The modeling procedure presented can be used to test excavation strategies in relation to hypothesized scenarios of stratigraphic evolution for archaeological sites.

SUPPLEMENTARY MATERIAL

Supplementary material in the form of 3D animations is available.

REFERENCES

Bettis, E.A., & Mandel, R.D. (2002). The effects of temporal and spatial patterns of Holocene erosion and alleviation on the archaeological record of the central and eastern Great Plains, USA. Geoarchaeology, 17, 141–154.

Bornholdt, S., Nordlund, U., & Westphal, H. (1999). Inverse stratigraphic modeling using genetic algorithms. In Harbaugh, W.L. Watney, E.C. Rankey, R. Slingerland, R.H. Goldstein, & E.K. Franseen (Eds.), Numerical experiments in stratigraphy: Recent advances in stratigraphic and sedimentologic computer simulations (pp. 85–90). SEPM Special Publication 62. Tulsa, OK: Society for Sedimentary Geology.

Brakenridge, G.R. (1980). Widespread episodes of stream erosion during the Holocene and their climatic cause. Nature, 283, 655–656.

Brown, A.G. (1997). Alluvial environments: Geoarchaeology and environmental change. Cambridge, UK: Cambridge University Press.

Bull, W.B. (1979). Threshold of critical power in streams. Geological Society of America, 90, 453–464.

Bull, W.B. (1991). Geomorphic responses to climatic change. Oxford: Oxford University Press.

Clevis, Q., de Boer, P.L., & Nijman, W. (2004) Differentiating the effect of episodic tectonism and eustatic sea-level fluctuations in foreland basins filled by alluvial fans and axial deltaic systems: Insights from a three-dimensional stratigraphic forward model. Sedimentology, 51, 809–835.

Clevis, Q., Tucker, G.E., Lock, G., & Desitter, A. (2004). Modeling the stratigraphy and geoarchaeology of English valley systems. Project report 3299. London: English Heritage.

Clevis, Q., Tucker, G.E., Lancaster, S.T., Desitter, A., Gasparini, N., & Lock, G. (2006). A simple algorithm for the mapping of TIN data onto a static grid: Applied to the stratigraphic simulation of river meander deposits. Computers and Geosciences, 32(6), 749–766.

Cross, T.A., & Lessenger, M.A. (1999). Construction and application of a stratigraphic inverse model. In J.W Harbaugh, W.L. Watney, E.C. Rankey, R. Slingerland, R.H. Goldstein, & E.K. Franseen (Eds.), Numerical experiments in stratigraphy: Recent advances in stratigraphic and sedimentologic computer simulations (pp. 62–83). SEPM Special Publication 62. Tulsa, OK: Society for Sedimentary Geology.

Dahl, S.O., & Nesje, A. (1996). A new approach to calculating Holocene winter precipitation by combining glacier equilibrium line altitudes and pine-tree limits: A case study from Hardangerlokulen, central southern Norway. Holocene, 6, 381–398.

Dean, J.S., Gumerman, G.J., Epstein, J.M., Axtell, R.L., Swedlund, A.C., Parker, M.T., et al. (2000). Understanding Anasazi culture change through agent-based modeling. In T.A. Kohler & G.J. Gumerman (Eds.), Dynamics in human and primate societies: Agent-based modeling of social and spatial processes (pp. 179–205). New York: Oxford University Press.

Dietrich, W.E., & Smith, J.D. (1983). Influence of the point bar on flow through curved channels. Water Resources Research, 19, 1173–1192.

Eagleson, P.S. (1978). Climate, soil, and vegetation: 2. The distribution of annual precipitation derived from observed storm sequences. Water Resources Research, 14, 713–721.

Gross, L.J., & Small, M.J. (1998). River and floodplain process simulation for subsurface characterization. Water Resource Research, 34, 2365–2376.

Guccione, M.J., Sierzchula, M.C., Lafferty, R.H., & Kelley, D. (1998). Site preservation along an active meandering and avulsing river: The Red River Kansas. Geoarchaeology, 13, 475–500.

Haas, J.N., Richoz, I., Tinner, W., & Wick, L. (1998). Synchonous Holocene climatic oscillations recorded on the Swiss Plateau and at the timber line in the Alps. The Holocene, 8, 301–309.

Hancock, G.S., & Anderson, R.S. (2002) Numerical modeling of fluvial terrace formation in response to oscillating climate. Geological Society of America Bulletin, 114, 1131–1142.

Howard, A.D. (1992). Modeling channel migration and floodplain sedimentation. In P.A. Carling & G.E. Petts (Eds.), Lowland floodplain rivers: Geomorphological perspectives (pp. 1–41). New York: Wiley.

Howard, A.D. (1996). Modeling channel evolution and floodplain morphology. In M.G. Anderson, D.E. Walling, & P.D. Bates (Eds.), Floodplain processes (pp. 15–62). Chichester: Wiley.

Huisink, M. (1997). Late Glacial sedimentological and morphological changes in a lowland river in response to climate change. Journal of Quarternary Science, 12, 209–223.

Johnson, W.C. (1999). Paleoenvironmental reconstruction at Fort Riley, Kansas (1998 phase). Champaign, IL: U.S. Army Construction Engineering Research Laboratories.

Johnson, W.C., & Logan, B. (1990). Geoarchaeology of the Kansas River basin, central Great Plains. In N.P. Lasca & J. Donohue (Eds.), Archaeological geology of North America (pp. 267–299). Geological Society of America, Decade of North American Geology Centennial Special Volume 4. Boulder, CO: Geological Society of America.

Johnson, W.C., & Zeidler, J.A. (1999). Modeling the potential for buried prehistoric archaeological remains on the Fort Riley military reservation, Kansas. Geological Society of America Abstracts with Programs, 31(5), 25.

Karssenberg, D., Tornqvist, T., & Bridge, J.S. (2001). Conditioning a process-based model of sedimentary architecture to well data. Journal of Sedimentary Research, 71, 868–879.

Kerr, B. (2004). Aggregates levy sustainability fund, annual report. London: English Heritage.

Kohler, T.A., Kresl, J., Van West, C.R., Carr, E., & Wilshusen, R. (2000). Be there then: A modeling approach to settlement determinants and spatial efficiency among late Ancestral Pueblo populations of the Mesa Verde region, U.S. Southwest. In T.A. Kohler & G.J. Gumerman (Eds.), Dynamics in human and primate societies: Agent-based modeling of social and spatial processes (pp. 145–178). New York: Oxford University Press.

Kohler, T.A., & Gumerman, G.J. (2000). Dynamics in human and primate societies: Agent-based modeling of social and spatial processes. New York: Oxford University Press.

Lake, M.W. (2000). MAGICAL computer simulation of Mesolithic foraging. In T.A. Kohler & G.J. Gumerman (Eds.), Dynamics in human and primate societies: Agent-based modeling of social and spatial processes (pp. 107–43). New York: Oxford University Press.

Lancaster, S.T., & Bras, R.L. (2002). A simple model of river meandering and its comparison to natural channels. Hydrological Processes, 16, 1–26.

Lancaster, S.T. (1998). A nonlinear river meander model and its incorporation in a landscape evolution model. Unpublished doctoral dissertation, Massachussets Institute of Technology, Cambridge, MA.

Mäckel, R., Schneider, R., & Seidel, J. (2003). Anthropogenic impact on the landscape of Southern Badenia (Germany) during the Holocene—Documented by colluvial and alluvial sediments. Archeometry, 45, 487–501.

Macklin, M.G., & Lewin, J. (2003). River sediments, great floods, and centennial-scale Holocene climate change. Journal of Quaternary Science, 18, 101–105.

Mackey, S.D., & Bridge, J.S. (1995). Three-dimensional model of alluvial stratigraphy: Theory and application. Journal of Sedimentary Research, B65, 7–31.

Oualine, S. (1997). Practical C programming (3rd ed.). Cambridge, MA: O'Reilly.

Pizzuto, J.E. (1987). Sediment diffusion during overbank flows. Sedimentology, 34, 301–317.

Schulz, M., & Paul, A. (2002). Holocene climate variability on centennial-to-millennial time scales: Climate records from the North-Atlantic realm. In G. Wefer, W. Berger, K.-E. Behre, E. Jansen (Eds.), Climate development and history of the North Atlantic realm (pp. 41–54). Berlin: Springer-Verlag.

Smith, J.D., & McLean, S.R. (1984). A model for flow in meandering streams. Water Resources Research, 20, 130–1315.

Snow, R.S., & Slingerland, R.L. (1987). Mathematical modeling of graded river profiles. Journal of Geology, 95, 15–33.

Starkel, L. (1988). Tectonic, anthropogenic and climatic factors in the history of the Vitula river valley downstream of Cracow. In G. Lang & C. Schluchter (Eds.), Lake, mire and river environments during the last 15000 years (pp. 161–170). Rotterdam: Balkema.

Stølum, H.-H., & Friend, P. (1997). Percolation theory applied to simulated meander belt sand bodies. Earth and Planetary Science Letters, 3–4, 265–277.

Tebbens, L.A., Veldkamp, A., Westerhoff, W., & Kroonenberg, S.B. (1999). Fluvial incision and channel downcutting as a response to Late-Glacial and Early Holocene climate change: The lower reach of the River Meuse (Maas). The Netherlands Journal of Quarternary Science, 14, 59–75.

Törnqvist, T.E., Wallinga, J., Murray, A.S., De Wolf, H., Cleveringa, P., & De Gans, W. (2000). Response of the Rhine-Meuse system (west-central Netherlands) to the last Quaternary glacio-eustatic cycles: A first assessment. Global and Planetary Change, 27, 89–111.

Tucker, G.E., & Bras, R.L. (2000). A stochastic approach to modeling the role of rainfall variability in drainage basin evolution. Water Resources Research, 36, 1953–1964.

Tucker, G.E., Lancaster, S.T., Gasparini, N.M., Bras, R.L., & Rybarczyk, S. (2001a.). An object-oriented framework for distributed hydrological modeling using triangular irregular networks. Computers and Geosciences, 27, 959–973.

Tucker, G.E., Lancaster, S.T., Gasparini, N.M., & Bras, R.L. (2001b). The channel-hillslope integrated landscape development model (CHILD). In W.W. Doe (Ed.), Landscape erosion and sedimentation modeling (pp. 349–388). New York: Springer.

Tucker, G.E. (2004). Drainage basin sensitivity to tectonic and climatic forcing: Implications of a stochastic model for the role of entrainment and erosion thresholds. Earth Surface Processes and Landforms, 29, 185–205.

Vandenberghe, J. (1995). Timescales, climate and river development. Quaternary Science Reviews, 14, 631–638

Verhulst, P.F. (1838). Notice sur la loi que la population suit dans son accroissement. Correspondence Mathématique et Physique, 10, 113–121.

Wainwright, J. (1994). Erosion of archaeological sites: Results and implications of a site simulation model. Geoarchaeology, 9, 173–201.

Walker, I.J., Desloges, J.R., Crawford, G., & Smith, D. (1997). Floodplain formation processes and archaeological implications at the Grand Banks site, lower Grand River, southern Ontario. Geoarchaeology, 12, 865–887.

Ward, I., & Larcombe, P. (2003). A process-oriented approach to archaeological site formation: Application to semi-arid northern Australia. Journal of Archaeological Science, 30, 1223–1236.

Waters, M.R. (2000). Alluvial stratigraphy and geoarchaeology in the American Southwest. Geoarchaeology, 15, 537–557.

Waters, M.R., & Kuehn, D.D. (1996). The Geoarchaeology of place: The effect of geological processes on the preservation and interpretation of the archaeological record. American Antiquity, 61, 483–497.

Wen, R. (2004). 3D modeling of stratigraphic heterogeneity in channelized reservoirs, methods and applications in seismic attributes facies classification. Canadian Society of Exploration Geophysicists Recorder, 3, 39–45.

White, A. (2000). Archaeological predictive modeling of site location through time: An example from the Tucson Basin, Arizona. Unpublished master's thesis, University of Calgary, Calgary, Canada.

Zeidler, J.A., & Isaacson, J.S. (1999). Managing buried archaeological sites on military training lands. In J.A. Zeidler (Ed.), Dynamic modeling of landscape evolution and archaeological site distributions: A three-dimensional approach (pp. 1–15). Center for Environmental Management of Military Lands, Technical Report TPS 01-8. Fort Collins, CO: Colorado State University.